

Structures and Reactivity of $(C_5H_4Me)_2Zr(CH_2CH_2R)(CH_3CN)_n^+$ Complexes. Competition between Insertion and β -H Elimination

Yun W. Alelyunas, Zhaoyu Guo, Robert E. LaPointe, and Richard F. Jordan*

Department of Chemistry, University of Iowa, Iowa City, Iowa 52242

Received June 15, 1992

A series of cationic alkyl complexes $(C_5H_4Me)_2Zr(CH_2CH_2R)(CH_3CN)_n^+$ (**3b,c**-**7b,c**; R = H, CH₃, CH₂CH₃, Ph, CMe₃) is generated by reaction of the corresponding THF complexes $(C_5H_4Me)_2Zr(CH_2CH_2R)(THF)^+$ (**3a**-**7a**) with excess CH₃CN. In CD₂Cl₂ these complexes exist as equilibrium mixtures of rapidly exchanging mono(CH₃CN) species (**3b**-**7b**) and bis(CH₃CN) species (**3c**-**7c**). K_{eq} for CH₃CN dissociation from the ethyl complex **3c** is estimated to be 0.5(3) M (20 °C) from the variation of ¹H NMR ethyl chemical shifts vs [CD₃CN]. NMR data establish that the mono(nitrile) ethyl complexes **3b** and $(C_5H_4Me)_2Zr(CH_2CH_3)(tBuCN)^+$ (**12**) adopt β -agostic structures analogous to those of $(C_5H_4Me)_2Zr(CH_2CH_2R)(PMe_3)^+$ species. Key data include high-field ¹H and ¹³C ZrCH₂CH₃ resonances, large $J_{C\alpha-H}$ values, and reduced $J_{C\alpha-C\beta}$ values (27 Hz). The J values are similar to values for cyclobutanes and thus reflect the reduced Zr-C-C and C-C-H_{br} angles and concomitant hybridization changes associated with the β -agostic structure, rather than extensive distortion toward an olefin hydride structure. By analogy to $(C_5H_4Me)_2Zr(CH_2CH_2R)(PMe_3)^+$ systems, the higher alkyls **4b**-**7b** also likely adopt β -agostic structures. In CD₂Cl₂ solution containing excess CH₃CN as a trapping reagent, **4b,c**-**7b,c** undergo clean β -H elimination and subsequent rapid CH₃CN insertion at 23 °C to yield $(C_5H_4Me)_2Zr\{N=C(H)(Me)\}(CH_3CN)^+$ (**11**) and olefin. Under these conditions, ethyl system **3b,c** undergoes competitive CH₃CN insertion leading to $(C_5H_4Me)_2Zr\{N=C(Et)(Me)\}(CH_3CN)^+$ (**10**, 84%) and β -H elimination leading to **11** (16%). Kinetic studies support a mechanism in which mono-(CH₃CN) complex **3b** undergoes competitive insertion and β -H elimination followed by rapid trapping; $k_{insert} = 4.38(9) \times 10^{-4} s^{-1}$ and $k_{\beta-elim} = 8.20(13) \times 10^{-5} s^{-1}$ at 20.0(4) °C. Kinetic studies of the reaction of ZrCH₂CH₂^tBu system **7b,c** support an analogous mechanism in which mono-(CH₃CN) complex **7b** undergoes rate-limiting β -H elimination ($k_{\beta-elim} = 9.4(1) \times 10^{-4} s^{-1}$) and $k_{insert} \ll k_{\beta-elim}$. Alkyl/aryl substituents on the β -carbon of $(C_5H_4Me)_2Zr(CH_2CH_2R)(CH_3CN)^+$ influence both insertion and β -H elimination rates.

Introduction

There is considerable evidence that 14-electron, d⁰ Cp₂M(R)⁺ cations are the active species in Cp₂MX₂-based olefin polymerization catalysts.^{1,2} Sixteen-electron Cp₂M(R)(L)⁺ complexes have been studied extensively as precursors to base-free species (via L dissociation)^{3,4} and

as models for Cp₂M(R)(substrate)⁺ intermediates.^{5,6} The insertion, β -H elimination, and σ -bond metathesis chemistry of these complexes is of interest for understanding the reaction mechanisms and structure/reactivity trends of Cp₂M(R)⁺ species in more complex catalyst systems, and for the development of other C-C bond forming reactions.^{7,8}

The nitrile insertion chemistry of Cp₂M(CH₃)(L)⁺ (M = Zr, Ti) complexes has been studied in detail (eqs 1 and 2). Nitriles are convenient substrates for mechanistic studies because the initial adducts can be directly observed or isolated, and only single insertions yielding stable M-N=CR₂ azaalkenylidene products occur. NMR and kinetics studies of the Zr system establish that the bis-

(1) For a review with extensive references see: Jordan, R. F. *Adv. Organomet. Chem.* 1991, 32, 325.

(2) For base-base Cp₂M(R)⁺ species see: (a) Eisch, J. J.; Piotrowski, A. M.; Brownstein, S. K.; Gabe, E. J.; Lee, F. L. *J. Am. Chem. Soc.* 1985, 107, 7219. (b) Hlatky, G. G.; Turner, H. W.; Eckman, R. R. *J. Am. Chem. Soc.* 1989, 111, 2798. (c) Christ, C. S., Jr.; Eyley, J. R.; Richardson, D. E. *J. Am. Chem. Soc.* 1990, 112, 596. (d) Lin, Z.; LeMarchal, J.-F.; Sabat, M.; Marks, T. J. *J. Am. Chem. Soc.* 1987, 109, 4127. (e) Bochmann, M.; Jagger, A. J.; Nicholls, J. C. *Angew. Chem., Int. Ed. Engl.* 1990, 29, 780. (f) Horton, A. D.; Orpen, A. G. *Organometallics* 1991, 10, 3910. (g) Yang, X.; Stern, C. L.; Marks, T. J. *Organometallics* 1991, 10, 840. (h) Ewen, J. A.; Elder, M. J.; Jones, R. L.; Haspelslagh, L.; Atwood, J. L.; Bott, S. G.; Robinson, K. *Makromol. Chem., Macromol. Symp.* 1991, 48/49, 253. (i) Hlatky, G. G.; Eckman, R. R.; Turner, H. W. *Organometallics* 1992, 11, 1413. (j) Horton, A. D.; Orpen, A. G. *Organometallics* 1992, 11, 8. See also: (k) Crowther, D. J.; Baenziger, N. C.; Jordan, R. F. *J. Am. Chem. Soc.* 1991, 113, 1455. (l) Chien, Tsai, W. M.; Rausch, M. D. *J. Am. Chem. Soc.* 1991, 113, 8570. (m) Yang, X.; Stern, C. L.; Marks, T. J. *J. Am. Chem. Soc.* 1991, 113, 362. (n) Bochmann, M.; Jagger, A. J. *J. Organomet. Chem.* 1992, 424, C5.

(3) (a) Jordan, R. F.; Dasher, W. E.; Echols, S. F. *J. Am. Chem. Soc.* 1986, 108, 1718. (b) Jordan, R. F.; Bajgur, C. S.; Willett, R.; Scott, B. *J. Am. Chem. Soc.* 1986, 108, 7410. (c) Jordan, R. F.; LaPointe, R. E.; Bajgur, C. S.; Willett, R. *J. Am. Chem. Soc.* 1987, 109, 4111. (d) Borkowsky, S. L.; Jordan, R. F.; Hinch, G. D. *Organometallics* 1991, 10, 1268.

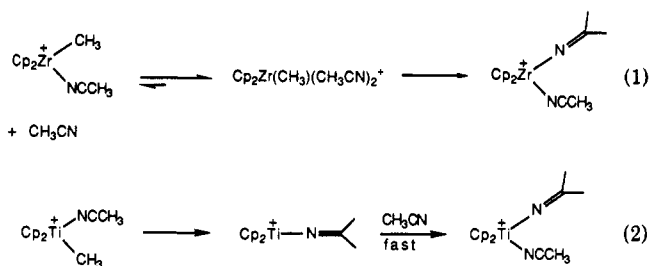
(4) (a) Eshuis, J. J. W.; Tan, Y. Y.; Teuben, J. H. *J. Mol. Catal.* 1990, 62, 277. (b) Eshuis, J. J. W.; Tan, Y. Y.; Meetsma, A.; Teuben, J. H. *Organometallics* 1992, 11, 362.

(5) (a) Jordan, R. F.; Bradley, P. K.; Baenziger, N. C.; LaPointe, R. E. *J. Am. Chem. Soc.* 1990, 112, 1289. (b) Jordan, R. F.; LaPointe, R. E.; Baenziger, N. C.; Hinch, G. D. *Organometallics* 1990, 9, 1539. (c) Wang, Y.; Jordan, R. F.; Bradley, P. K.; Baenziger, N. C. *Polym. Prepr. (Am. Chem. Soc., Div. Polym. Chem.)* 1991, 32, 457.

(6) (a) Bochmann, M.; Wilson, L. M.; Hursthouse, M. B.; Short, R. L. *Organometallics* 1987, 6, 2556. (b) Taube, R.; Krukowa, L. *J. Organomet. Chem.* 1988, 347, C9.

(7) (a) Jordan, R. F.; Bajgur, C. S.; Dasher, W. E.; Rheingold, A. L. *Organometallics* 1987, 6, 1041. (b) Jordan, R. F.; LaPointe, R. E.; Bradley, P. K.; Baenziger, N. *Organometallics* 1989, 8, 2892. (c) Guram, A. S.; Jordan, R. F. *Organometallics* 1990, 9, 2190.

(8) (a) Jordan, R. F.; Guram, A. S. *Organometallics* 1990, 9, 2116. (b) Jordan, R. F.; Taylor, D. F. *Organometallics* 1990, 9, 1546. (c) Jordan, R. F.; Taylor, D. F. *J. Am. Chem. Soc.* 1989, 111, 778. (d) Jordan, R. F.; Bradley, P. F.; LaPointe, R. E.; Taylor, D. F. *New J. Chem.* 1990, 14, 505. (e) Guram, A. S.; Jordan, R. F. *Organometallics* 1991, 10, 3470. (f) Guram, A. S.; Jordan, R. F. *J. Org. Chem.* 1992, 57, 5994.

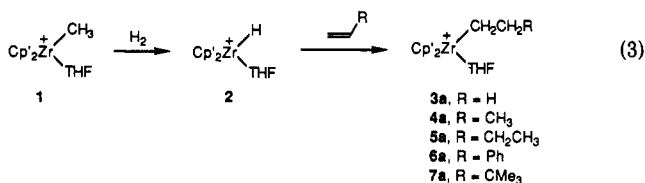


(nitrile) adduct $Cp_2Zr(CH_3)(CH_3CN)_2^+$ is strongly favored over the mono(nitrile) adduct and undergoes insertion (eq 1) and that electron-donor groups on the Cp ring accelerate this process.⁹ In contrast, bis(nitrile) adducts are not observed in the Ti system, and the mono adducts undergo rate-limiting insertion followed by rapid trapping (eq 2).¹⁰

In this paper, the structures and reactivity with CH_3CN of higher alkyl complexes, $Cp'_2Zr(CH_2CH_2R)(CH_3CN)_n^+$ ($Cp' = C_5H_4Me$), are described. For these systems β -H elimination becomes a dominant process. The counterion is BPh_4^- in all cases.

Results and Discussion

Synthesis and Solution Structures of $Cp'_2Zr(CH_2CH_2R)(L)^+$ ($L = THF, PMe_3$) Complexes. Hydrogenolysis of $Cp'_2Zr(CH_3)(THF)^+$ (1) yields $Cp'_2Zr(H)(THF)^+$ (2), which provides general access to cationic alkyl complexes $Cp'_2Zr(CH_2CH_2R)(THF)^+$ (3a-7a) via reaction with the appropriate olefin as described previously (eq 3).^{7b} The alkyl groups of these complexes adopt normal,

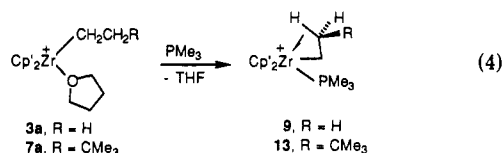


undistorted structures. Key NMR spectroscopic parameters for ethyl complex 3a, which are characteristic of normal ethyl ligands in $Cp'_2Zr(CH_2CH_2R)(L)^+$ systems, include (i) a low-field H_β resonance (δ 1.42) which is downfield of the H_α resonance (δ 1.23), (ii) normal ^{13}C parameters for C_β (δ 17.1, $J_{CH} = 125$ Hz), and (iii) slightly reduced J_{CH} value for C_α (δ 60.7, $J_{CH} = 116$ Hz) due to the electropositive Zr.¹¹ The ^{13}C -labeled complex $Cp'_2Zr(^{13}CH_2^{13}CH_3)(THF)^+$ (3a- $^{13}C_2$) was prepared by reaction of $Cp'_2Zr(H)(THF)^+$ with ethylene- $^{13}C_2$ and $J_{C_\alpha-C_\beta}$ determined (32.9 Hz). This value is slightly lower than J_{CC} for ethane (34.6 Hz).¹²

Complex 3a is stable in THF but decomposes slowly in CH_2Cl_2 to the known $Cp'_2Zr(CH_2CH_3)Cl$ (8) by chloride abstraction.¹³ The formation of 8 was confirmed via an independent preparation from 3a and $[NMe_4]Cl$. The spectroscopic properties of 8 are similar to those of 3a and

are consistent with a normal, undistorted ethyl group (Table I). As for 3a, the H_β resonance (δ 1.29) is downfield of the H_α resonance (δ 0.88), the ^{13}C parameters for C_β are normal (δ 17.9, $J_{CH} = 124$ Hz), the $J_{C_\alpha-H}$ value (118 Hz) is slightly reduced from the normal sp^3 value, and $J_{C_\alpha-C_\beta}$ (32.3 Hz, measured for 8- $^{13}C_2$) is slightly less than the value for ethane.

Reaction of 3a-7a with PMe_3 generates the PMe_3 complexes $Cp'_2Zr(CH_2CH_2R)(PMe_3)^+$ which adopt agostic structures¹⁴ with a single β -H bridging to Zr (X-ray, 1H , ^{13}C NMR, isotopic perturbation of resonance, IR), as described in detail elsewhere^{5,15} and as shown for 3a and 7a in eq 4. Exchange of terminal and bridging β -hydrogens is rapid on the NMR time scale for these systems.



It is useful to summarize here the key NMR spectroscopic properties for ethyl derivative 9 (Table I), which are characteristic of β -agostic ethyl ligands in $Cp'_2Zr(CH_2CH_2R)(L)^+$ species. Key data for 9 include (i) a high-field H_β resonance (δ -1.26, at 23 °C) which is upfield of the H_α resonance (δ 0.91), (ii) a relatively high-field chemical shift and large C-H coupling constant for C_α (δ 28.6, $J_{CH} = 141$ Hz), (iii) a high-field C_β resonance (δ -6.9, $J_{CH} = 123$ Hz), and (iv) a reduced $J_{C_\alpha-C_\beta}$ value (28.5 Hz, determined for 9- $^{13}C_2$). The last value is similar to J_{CC} values for cyclobutanes (ca. 29 Hz)¹⁶ and much smaller than that of ethylene (67.6 Hz),¹⁷ and thus reflects the reduced Zr-C-C and C-C-H_{br} angles and concomitant hybridization changes associated with the agostic structure rather than extensive distortion toward an olefin hydride structure.^{14a,18,19} Spencer has noted reduced J_{CC} values for cationic, β -agostic Pt complexes $(PP)Pt(Et)^+$ ($PP = o$ -(t Bu)₂PCH₂)₂C₆H₄, $J_{CC} = 29$ Hz; $PP = (^t$ Bu)₂P(CH₂)₃P-(t Bu)₂, $J_{CC} = 26$ Hz).²⁰ Also, Brookhart's group has found that J_{CC} is small (29 Hz) for the β -agostic Co cations $Cp^*Co\{P(OMe)_3\}CHRCH_3^+$, but larger (36-39 Hz) for the isomeric species $Cp^*Co\{P(OMe)_3\}CH_2CH_2R^+$ which are more strongly distorted toward olefin hydride structures.²¹ The $J_{C_\alpha-H}$ value for 9 is also similar to that of cyclobutane (134 Hz) and can be ascribed to the reduced Zr-C-C angle.²² The $J_{C_\beta-H}$ value is the weighted average (due to the rapid

(14) Reviews: (a) Brookhart, M.; Green, M. L. H.; Wong, L. *Prog. Inorg. Chem.* 1988, 36, 1. (b) Crabtree, R. H.; Hamilton, D. G. *Adv. Organomet. Chem.* 1988, 28, 299.

(15) Bradley, P. K.; Alelyunas, Y. W.; Guo, Z.; Jordan, R. F. Manuscript in preparation.

(16) Reported values for methylcyclobutane are $J_{C_1-C_2} = 29.1$ Hz, $J_{C_2-C_3} = 28.4$ Hz. Stocker, M.; Klessinger, M. *Org. Magn. Reson.* 1979, 12, 107.

(17) Weigert, F. J.; Roberts, J. D. *J. Am. Chem. Soc.* 1971, 94, 6021.

(18) The Zr-C-C angle in 9 (84.7°)^{5a} is similar to that in cyclobutane (87.2°). (a) Almennigen, A.; Bastiansen, O.; Skanke, P. N. *Acta Chem. Scand.* 1961, 15, 711. (b) Wiberg, K. B. *J. Am. Chem. Soc.* 1983, 105, 1227.

(19) See also discussions in: (a) Thompson, M. E.; Baxter, S. M.; Bulls, A. R.; Burger, B. J.; Nolan, M. C.; Santarsiero, B. D.; Schaefer, W. P.; Bercaw, J. E. *J. Am. Chem. Soc.* 1987, 109, 203. (b) Bender, B. R.; Norton, J. R.; Miller, M. M.; Anderson, O. P.; Rappé, A. K. *Organometallics*, in press.

(20) Mole, L.; Spencer, J. L.; Carr, N.; Orpen, A. G. *Organometallics* 1991, 10, 49.

(21) (a) Volpe, T. Ph.D. Thesis, University of North Carolina, 1991. (b) M. Brookhart, personal communication.

(22) (a) Yonezawa, T.; Moreschima, I.; Fujii, M.; Fuki, K. *Bull. Chem. Soc. Jpn.* 1965, 38, 1226. (b) Aydin, R.; Gunther, H. *J. Am. Chem. Soc.* 1981, 103, 1301.

(9) Alelyunas, Y. W.; Jordan, R. F.; Echols, S. F.; Borkowsky, S. L.; Bradley, P. K. *Organometallics* 1991, 10, 1406.

(10) Bochmann, M.; Wilson, L. M.; Hursthouse, M. B.; Motevalli, M. *Organometallics* 1988, 7, 1148.

(11) (a) Yoder, C. H.; Tuck, R. H.; Hess, R. G. *J. Am. Chem. Soc.* 1969, 91, 539. (b) McKeever, L. D.; Waack, R.; Doran, M. A.; Baker, E. B. *J. Am. Chem. Soc.* 1969, 91, 1057. (c) Fraenkel, G.; Adams, D. G.; Williams, J. *Tetrahedron Lett.* 1963, 767. (d) Finch, W. C.; Anslyn, E. V.; Grubbs, R. H. *J. Am. Chem. Soc.* 1988, 110, 2406.

(12) Summerhays, K. D.; Maceil, G. E. *J. Am. Chem. Soc.* 1972, 94, 8348.

(13) Erker, G.; Schlund, R.; Kruger, C. *Organometallics* 1989, 8, 2349.

Table I. NMR Data^a

compd (solvent)	¹ H, δ	assign	¹³ C, δ	assign
Cp' ₂ Zr(CH ₂ CH ₃)(THF) ⁺ (3a) (CD ₂ Cl ₂)	6.07–6.15 (m, 8 H)	C ₅ H ₄ Me	60.7 (td, J _{CH} = 116, J _{CC} = 32.9) ^d	ZrCH ₂
	3.46 (m, 4 H)	O(CH ₂ CH ₂) ₂	17.7 (qd, J _{CH} = 125, J _{CC} = 32.9) ^d	CH ₂ CH ₃
	2.14 (s, 6 H)	C ₅ H ₄ CH ₃		
	1.83 (m, 4 H)	O(CH ₂ CH ₂) ₂		
	1.42 (t, 3 H)	CH ₂ CH ₃		
Cp' ₂ Zr(CH ₂ CH ₃)(CH ₃ CN) ⁺ (3b) (CD ₂ Cl ₂ , -40 °C)	1.23 (q, 2 H)	ZrCH ₂		
	5.95 (m, 8 H)	C ₅ H ₄ Me	39.49 (td, J _{CH} = 139, J _{CC} = 26.9) ^d	ZrCH ₂
	2.00 (s, 6 H)	C ₅ H ₄ CH ₃	-0.29 (qd, J _{CH} = 124, J _{CC} = 26.9) ^d	CH ₂ CH ₃
	1.47 (q, J = 8.6, 2 H)	ZrCH ₂		
	1.32 (s, 3 H)	CH ₃ CN		
Cp' ₂ Zr(CH ₂ CH ₃)(CD ₃ CN) _n ⁺ b,c (3c) (CD ₃ CN)	0.07 (t, J = 8.6, 3 H)	CH ₂ CH ₃		
	5.93 (m, 4 H)	C ₅ H ₄ Me	40.5 (td, J _{CH} = 119, J _{CC} = 33) ^d	ZrCH ₂
	5.81 (m, 4 H)	C ₅ H ₄ Me	17.1 (qd, J _{CH} = 123, J _{CC} = 33) ^d	CH ₂ CH ₃
	3.64 (m, 4 H)	O(CH ₂ CH ₂) ₂		
	2.12 (s, 6 H)	C ₅ H ₄ CH ₃		
	1.83 (m, 4 H)	O(CH ₂ CH ₂) ₂		
Cp' ₂ Zr(CH ₂ CH ₂ Ph)(CH ₃ CN) _n ⁺ (6c) (CD ₃ CN, -40 °C)	1.21 (t, 3 H)	CH ₂ CH ₃		
	0.77 (q, 2 H)	ZrCH ₂		
	6.7–7.4 (m, 25 H)	Ph, BPh ₄ ⁻		
	6.00 (m, 4 H)	C ₅ H ₄ Me		
	5.83 (m, 4 H)	C ₅ H ₄ Me		
	2.61 (AA'XX', 2 H)	CH ₂ Ph		
	2.10 (s, 6 H)	C ₅ H ₄ CH ₃		
	0.90 (AA'XX', 2 H)	ZrCH ₂		
	6.21 (m, 4 H)	C ₅ H ₄ Me	129.9	(CH) ₄ CCH ₃
	6.14 (m, 4 H)	C ₅ H ₄ Me	116.4	(CH) ₄ CCH ₃
Cp' ₂ Zr(CH ₂ CH ₂ ^t Bu)(THF) ⁺ (7a) (THF-d ₆)	2.11 (s, 6 H)	C ₅ H ₄ CH ₃	114.4	(CH) ₄ CCH ₃
	1.50 (AA'XX', 2 H)	CH ₂ ^t Bu	64.4	ZrCH ₂
	1.18 (AA'XX', 2 H)	ZrCH ₂	48.0	CMe ₃
	0.88 (s, 9 H)	C(CH ₃) ₃	33.5	CH ₂ ^t Bu
			29.2	C(CH ₃) ₃
			14.7	(CH) ₄ CH ₃
Cp' ₂ Zr(CH ₂ CH ₂ ^t Bu)(THF) ⁺ (7a) (CD ₂ Cl ₂ , -33 °C)	6.10 (m, 4 H)	C ₅ H ₄ Me		
	6.01 (m, 4 H)	C ₅ H ₄ Me		
	3.37 (m, 4 H)	O(CH ₂ CH ₂) ₂		
	2.12 (s, 6 H)	C ₅ H ₄ CH ₃		
	1.80 (m, 4 H)	O(CH ₂ CH ₂) ₂		
	1.40 (AA'XX', 2 H)	CH ₂ ^t Bu		
	1.17 (AA'XX', 2 H)	ZrCH ₂		
	0.83 (s, 9 H)	C(CH ₃) ₃		
Cp' ₂ Zr(CH ₂ CH ₂ ^t Bu)(NCCD ₃) _n ⁺ b (7c) (CD ₃ CN, ¹³ C at -20 °C)	5.92 (m, 4 H)	C ₅ H ₄ Me	123.1	(CH) ₄ CCH ₃
	5.80 (m, 4 H)	C ₅ H ₄ Me	115.6	(CH) ₄ CCH ₃
	3.64 (m, 4 H)	O(CH ₂ CH ₂) ₂	108.0	(CH) ₄ CCH ₃
	2.12 (s, 6 H)	C ₅ H ₄ CH ₃	48.0	ZrCH ₂
	1.80 (m, 4 H)	O(CH ₂ CH ₂) ₂	42.1	CMe ₃
	1.26 (AA'XX', 2 H)	CH ₂ ^t Bu	33.5	CH ₂ CMe ₃
	0.85 (s, 9 H)	C(CH ₃) ₃	29.1	C(CH ₃) ₃
	0.71 (AA'XX', 2 H)	ZrCH ₂	14.6	(CH) ₄ CCH ₃
Cp' ₂ Zr(CH ₂ CH ₃)Cl (8) (CD ₂ Cl ₂ , 25 °C)	6.09 (m, 4 H)	C ₅ H ₄ Me	45.5 (td, J _{CH} = 118, J _{CC} = 32.3) ^d	ZrCH ₂
	6.02 (m, 4 H)	C ₅ H ₄ Me	17.9 (qd, J _{CH} = 124, J _{CC} = 32.3) ^d	CH ₂ CH ₃
	2.21 (s, 6 H)	C ₅ H ₄ CH ₃		
	1.29 (t, J = 7, 3 H)	CH ₂ CH ₃		
	0.88 (q, J = 7, 3 H)	ZrCH ₂		
Cp' ₂ Zr(CH ₂ CH ₃)(PMe ₃) ⁺ (9)	5.74 (m, 2 H)	C ₅ H ₄ Me	28.6 (td, J _{CH} = 141, J _{CC} = 28.5) ^d	ZrCH ₂
	5.59 (m, 2 H)	C ₅ H ₄ Me	-6.9 (qd, J _{CH} = 123, J _{CC} = 28.5) ^d	CH ₂ CH ₃
	5.53 (m, 2 H)	C ₅ H ₄ Me		
	5.49 (m, 2 H)	C ₅ H ₄ Me		
	1.98 (s, 6 H)	C ₅ H ₄ CH ₃		
	1.36 (d, J _{PH} = 7.6, 9 H)	P(CH ₃) ₃		
	0.91 (dq, J _{HH} = 8.4, J _{PH} = 8.6, 2 H)	ZrCH ₂		
	-1.26 (dt, J _{HH} = 8.6, J _{PH} = 4.5, 3 H)	CH ₂ CH ₃		
Cp' ₂ Zr{N=C(CH ₃)(CH ₂ CH ₃)}(CH ₃ CN) ⁺ (10) (CD ₂ Cl ₂ , isomer ratio 3:1)	5.99 (br s, 2 H)	C ₅ H ₄ Me	183.5	=C(Me)(Et)
	5.93 (br s, 4 H)	C ₅ H ₄ Me	134.0	CH ₃ CN
	5.87 (br s, 2 H)	C ₅ H ₄ Me	126.4	(CH) ₄ CCH ₃
	2.27 (q, J = 7.3)	=CCH ₂ Me, major	112.8	(CH) ₄ CCH ₃
	2.24 (q, J = 7.3, 2 H ^r)	=CCH ₂ Me, minor	110.5 (t, 129)	(CH) ₄ CCH ₃
	2.05 (s, 6 H)	C ₅ H ₄ CH ₃	108.4	(CH) ₄ CCH ₃
	1.96 (s)	=C(CH ₃), major	108.2	(CH) ₄ CCH ₃
	1.90 (s, 3 H ^r)	=C(CH ₃), minor	34.5 (t, J = 125)	=CCH ₂ CH ₃
	1.63 (s)	CH ₃ CN, major	29.2 (q, J = 127)	=C(CH ₃)
	1.61 (s, 3 H ^r)	CH ₃ CN, minor	15.2 (q, J = 127)	(CH) ₄ CCH ₃
	1.05 (t, J = 7.3)	=CCH ₂ CH ₃ , minor	10.3 (q, J = 117)	=CCH ₂ CH ₃
	0.87 (t, J = 7.3, 3 H ^r)	=CCH ₂ CH ₃ , major	2.1 (q, J = 139)	CH ₃ CN

Table I (Continued)

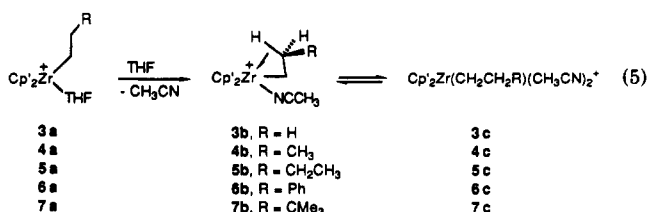
compd (solvent)	¹ H, δ	assign	¹³ C, δ	assign
Cp' ₂ Zr{N=C(CH ₃)(CH ₂ CH ₃)}(CH ₃ CN) ⁺ (10) (CD ₃ CN)	6.09 (m, 4 H)	C ₅ H ₄ Me	34.5 (J _{CC} = 36.0) ^d	=CCH ₂ CH ₃
	6.02 (m, 4 H)	C ₅ H ₄ Me	10.3 (J _{CC} = 36.0) ^d	=CCH ₂ CH ₃
	2.26 (q, J = 7.3, 2 H)	=CCH ₂ Me		
	2.05 (s, 6 H)	C ₅ H ₄ CH ₃		
	1.95 (s, 3 H)	=C(CH ₃)		
	1.93 (s, 3 H)	liberated CH ₃ CN		
Cp' ₂ Zr(CH ₂ CH ₃){(CH ₃) ₃ CCN} ⁺ (12) (CD ₂ Cl ₂ , -40 °C)	0.88 (t, J = 7.3, 3 H)	=CCH ₂ CH ₃		
	5.8–6.0 (m, 8 H)	C ₅ H ₄ Me	40.33 (td, J _{CH} = 137, J _{CC} = 26.9) ^d	ZrCH ₂
	2.05 (s, 6 H)	C ₅ H ₄ CH ₃	-1.11 (qd, J _{CH} = 123, J _{CC} = 26.9) ^d	CH ₂ CH ₃
	1.54 (m, 2 H)	ZrCH ₂		
	1.54 (s, 9 H)	(CH ₃) ₃ CCN		
	-0.03 (t, J = 8.5, 3 H)	CH ₂ CH ₃		
Cp' ₂ Zr(CH ₂ CH ₂ ^t Bu)(PMe ₃) ⁺ (14) (CD ₂ Cl ₂ , ¹³ C at -20 °C, contains 0.7 equiv excess of PMe ₃)	5.76 (m, 4 H)	C ₅ H ₄ Me	123.3	(CH) ₄ CCH ₃
	5.69 (m, 4 H)	C ₅ H ₄ Me	110.5	(CH) ₄ CCH ₃
	2.12 (s, 6 H)	C ₅ H ₄ CH ₃	105.5	(CH) ₄ CCH ₃
	1.20 (d, J = 1.2)	PMe ₃ , free PMe ₃	34.75 (t, J = 140)	ZrCH ₂
	0.94 (s, 9 H)	C(CH ₃) ₃	34.75 (t, J = 140)	ZrCH ₂
	0.91 (AA'XX', 2 H)	ZrCH ₂	32.73	CMe ₃
	-0.85 (AA'XX', 2 H)	CH ₂ Bu	29.77 (q, J = 128)	C(CH ₃) ₃
			24.36 (t, J = 113)	CH ₂ CMe ₃
			15.95 (q, J = 129)	(CH) ₄ CCH ₃
			15.01 (q, J = 128)	PMe ₃ , free PMe ₃

^a All spectra contain normal BPh₄⁻ resonances. Spectra are recorded at 23 °C unless indicated. For full ¹³C spectra of 3a, 8, and 9 see references cited in the text. J_{CH} values are from gated ¹³C spectra unless indicated. ^b The nitrile complex is obtained by dissolving the corresponding THF complex in CD₃CN. Therefore the number of coordinated CD₃CN is not known. ^c See text for the discussion. ^d From the corresponding ¹³C-labeled complexes. ^e Integral is total for major and minor isomer.

bridge-terminal exchange) of two large (terminal H) and one reduced (μ-H) values.

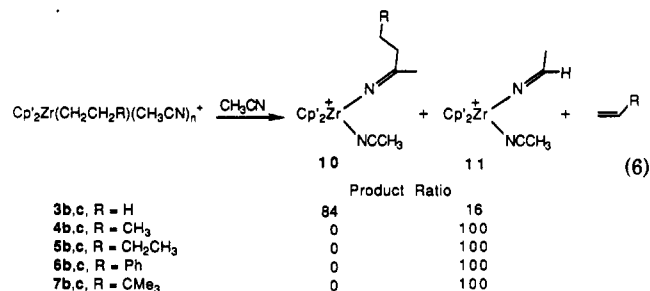
The previously unreported neohexyl complex 7a is isolated in 70% yield from the reaction of Cp'₂Zr(H)-(THF)⁺ with ^tBu-ethylene, and like 3a–6a, adopts a normal structure. Reaction of 7a with PMe₃ (1.7 equiv) yields the thermally sensitive PMe₃ complex Cp'₂Zr(CH₂CH₂^tBu)(PMe₃)⁺ (13, eq 4), which has been characterized by low-temperature NMR spectroscopy. Despite the bulky ^tBu substituent, 13 adopts a β-agostic structure in which exchange of terminal and bridging β-hydrogens is rapid on the NMR time scale. Key NMR data for 13 include (i) a high-field β-CH₂R resonance (δ = -0.85), which is *upfield* of the α-CH₂ resonance, (ii) a large J_{Cα-H} value (J = 140 Hz), and (iii) a reduced J_{Cβ-H} value (J = 111 Hz) which is the average of one large (terminal-H) and one small (μ-H) value. Comparison of the ¹H NMR spectra of 13 and Cp'₂Zr(CH₂CHDCMe₃)(PMe₃)⁺ (13-d₁) reveals a substantial, temperature-dependent isotopic perturbation of resonance (δ(ZrCH₂CH₂^tBu) - δ(Zr(CH₂CHD^tBu)) = 0.43 at -90 °C, 0.25 at -30 °C, and 0.19 at 0 °C).²³ Complex 13 undergoes rapid exchange with free PMe₃ at -20 °C and rapid β-H elimination at 20 °C.

Reactions of Cp'₂Zr(CH₂CH₂R)(THF)⁺ Complexes with CH₃CN. Dissolution of 3a, 6a, or 7a in neat CH₃CN or reaction with excess CH₃CN in CH₂Cl₂ solution at -40 or 20 °C results in immediate displacement of THF and the formation of thermally unstable CH₃CN complexes 3b,c, 6b,c, and 7b,c (eq 5). Monitoring these reactions by



¹H NMR reveals the immediate appearance of resonances for free THF and large shifts in the Cp' and CH₂CH₂R resonances consistent with ligand substitution (Table I). In general, exchange of free and coordinated CH₃CN is rapid on the NMR time scale for these systems, and thus the nature and number of coordinated CH₃CN ligands is not known. However, previous ¹H NMR and kinetic studies of the reaction of Cp₂Zr(CH₃)(THF)⁺ with CH₃CN under similar conditions (eq 1) establish that an equilibrium mixture of Cp₂Zr(CH₃)(CH₃CN)⁺ and Cp₂Zr(CH₃)(CH₃CN)₂⁺ (two isomers) is formed, with the bis-(nitrile) adduct strongly favored. We assume that both bis- (3c, 6c, 7c) and mono(CH₃CN) (3b, 6b, 7b) complexes are possible for the higher alkyls as well, as indicated in eq 5. This question is addressed in more detail for 3 and 7 in the following sections. The reactions of propyl and butyl complexes 4a and 5a with CH₃CN were investigated at ambient temperature only. Under these conditions, the presumed CH₃CN complexes undergo instantaneous β-H elimination (*vide infra*) and were not observed.

The CH₃CN complexes 3b,c–7b,c, generated *in situ* from 3a–7a, decompose by β-H elimination and/or CH₃CN insertion pathways to yield azaalkenylidene complexes (eq 6). Complexes 4b,c–7b,c, which contain alkyl or phenyl



substituents on the β-carbon, react cleanly in the presence of excess CH₃CN to yield Cp'₂Zr{N=C(H)(Me)}(CH₃CN)⁺ (11, >95% NMR yield), which was characterized previously,⁷ and the corresponding olefins (eq 6). The most likely pathway leading to these products is initial β-H

elimination to yield olefin and $\text{Cp}'_2\text{Zr}(\text{H})(\text{CH}_3\text{CN})_n^+$, which is known to undergo rapid CH_3CN insertion into the Zr—H bond.^{7a,b,24} NMR monitoring experiments in neat CD_3CN show that when $\text{R} = \text{CH}_3$ (**4**) and CH_2CH_3 (**5**), the reaction is complete within 10 min at 23 °C. The reaction of **7** with CD_3CN is much slower (75% complete in 5 h at 23 °C). The β -H elimination leading to **11** is observed as a minor process in the reaction of **3b,c** with excess CH_3CN . The major product in this case is $\text{Cp}'_2\text{Zr}\{\text{N}=\text{C}(\text{Et})(\text{Me})\}(\text{CH}_3\text{CN})^+$ (**10**) which is derived from direct insertion of CH_3CN into the Zr— CH_2CH_3 bond. The combined NMR yield of **10** and **11** from the reaction of **3b,c** is >95%.

Both the β -H elimination and the CH_3CN insertion reactions described above are inhibited by CH_3CN . For example, the reaction of phenethyl complex **6b,c** with 2 equiv of CH_3CN in CD_2Cl_2 solution (which produces **11** and styrene) is complete in less than 30 min at 10 °C, whereas reaction of **6** in neat CD_3CN at the same temperature has a $t_{1/2}$ of ca. 35 min. Similarly, the reaction of ethyl complex **3b,c** with 4 equiv of CD_3CN in CD_2Cl_2 solution at 15 °C (>50% complete after 1 h) is much faster than the analogous reaction in neat CD_3CN (ca. 60% complete after 5 h, 23 °C).

Characterization and Solution Behavior of $\text{Cp}'_2\text{Zr}(\text{CH}_2\text{CH}_3)(\text{CH}_3\text{CN})_n^+$ (3b**, $n = 1$; **3c**, $n = 2$).** Dissolution of **3a** in neat CH_3CN followed by removal of solvent as described in the Experimental Section yields the thermally sensitive bis(nitrile) adduct **3c**. The low-temperature (−40 °C) ^1H NMR spectrum of a solution of **3c** in CD_2Cl_2 containing 1.8 M CD_3CN (to inhibit conversion to **10** and **11**) contains a resonance for free, liberated CH_3CN (2 equiv). This establishes that the isolated solid contains 2 equiv of CH_3CN and that exchange between free and coordinated nitrile is fast on the laboratory time scale. ^1H NMR spectra of **3c** in CD_2Cl_2 containing excess CH_3CN exhibit only a single CH_3CN resonance consistent with rapid exchange on the NMR time scale. NMR data for **3c** (neat CD_3CN) are similar to those for **3a** and **8** and are consistent with a *normal* ethyl structure as expected for an 18- e^- complex. Key data include (i) a low-field H_β resonance (δ 1.21) which is downfield of the H_α resonance, (ii) normal ^{13}C parameters for C_β (δ 17.1, $J_{\text{CH}} = 123$ Hz) and C_α (δ 40.5, $J_{\text{CH}} = 119$ Hz), and (iii) a normal $J_{\text{C}_\alpha-\text{C}_\beta}$ value (33.0 Hz, measured for **3c- $^{13}\text{C}_2$**).

Isolation and full characterization of the mono(CH_3CN) adduct **3b** was precluded by its thermal instability and poor solubility properties. However this species can be obtained as an impure yellow solid by dissolution of **3c** in CH_2Cl_2 followed by removal of volatiles as described in the Experimental Section. Low-temperature NMR data (−40 °C, CD_2Cl_2) for **3b** are similar to those for PMe_3 complex **9** and establish that the ethyl ligand is distorted by a β -agostic interaction. Key data include: (i) a high-field H_β resonance (δ 0.07) which is *upfield* of the H_α resonance (δ 1.47), (ii) a large C—H coupling constant for C_α ($J_{\text{CH}} = 139$ Hz), (iii) a high-field C_β ^{13}C NMR resonance (δ −0.29), and (iv) a reduced $J_{\text{C}_\alpha-\text{C}_\beta}$ value (26.9 Hz). The mono(nitrile) complex **3b** is only sparingly soluble in neat CD_2Cl_2 but dissolves upon addition of 3.5 M of CD_3CN .

(24) (a) Direct β -H transfers to coordinated substrates (without the intermediacy of M—H species) have been discussed for Ti and V systems.^{b,c} Such a process cannot be definitively ruled out here but is considered unlikely as $\text{Cp}'_2\text{Zr}(\text{CH}_2\text{CH}_2\text{R})(\text{PMe}_3)^+$ complexes decompose by β -H elimination (in the presence of excess PMe_3) to the well-characterized hydride $\text{Cp}'_2\text{Zr}(\text{H})(\text{PMe}_3)_2^+$.^{5b} (b) Luinstra, G. A.; Teuben, J. H. *J. Chem. Soc., Chem. Commun.* 1987, 849. (c) Galanta, J. M.; Bruno, J. W.; Hazin, P. N.; Foltz, K.; Huffman, J. C. *Organometallics* 1988, 7, 1066.

Table II. Variation of $-\text{CH}_2\text{CH}_3$ ^1H NMR Parameters for **3** at Different $[\text{CD}_3\text{CN}]$ in CD_2Cl_2^a

entry	temp, °C	$[\text{CD}_3\text{CN}]$, M	$\delta(\text{H}_\alpha)$ (CH_2)	$\delta(\text{H}_\beta)$ (CH_3)
1	25 ^b	19.1	0.82	1.26
2	25	0.30	1.25	0.61
3	20	3.81	0.87	1.16
4	20	3.50	0.88	1.13
5	20	1.61	0.93	1.04
6	20	0.76	1.02	0.88
7	20	0.69	1.08	0.83
8	−40	5.45	0.71	1.15
9	−40	4.00	0.72	1.16
10	−40	2.26	0.76	1.16
11	−40	1.01	0.78	1.12
12	−40	0.70	0.81	1.08

^a Referenced to CHDCl_2 residual ^1H resonance. ^b **3a** in neat CD_3CN .

The ^1H NMR spectrum of the resulting solution (−40 °C) exhibits resonances for bis(CD_3CN) complex **3c-d₆** and liberated free CH_3CN (1 equiv). This experiment confirms that the isolated solid is a mono(CH_3CN) adduct and that the exchange between free and coordinated nitrile is fast on the laboratory time scale.

To confirm the β -agostic structure of mono(CH_3CN) adduct **3b**, we briefly investigated the synthesis of more soluble analogues containing bulky nitriles. The reaction of **3a** with Me_3CCN yields the soluble, thermally sensitive complex $\text{Cp}'_2\text{Zr}(\text{CH}_2\text{CH}_3)(\text{Me}_3\text{CCN})^+$ (**12**), which has been characterized by NMR spectroscopy at −40 °C (Table I). NMR data for **12** are very similar to data for mono(CH_3CN) adduct **3b** and PMe_3 complex **9** and thus confirm that the former has a β -agostic structure.²⁵

The ^1H NMR spectra of solutions of THF adduct **3a** in CD_2Cl_2 containing 0.7–3.5 M CD_3CN (the range used in kinetic studies; vide infra), exhibit resonances for free, liberated THF which shift only slightly with changing $[\text{CH}_3\text{CN}]$.²⁶ This is consistent with complete ligand exchange and conversion to **3b,c** under these conditions, as indicated in eq 5. However, the chemical shifts of H_α and H_β vary significantly with $[\text{CD}_3\text{CN}]$ and temperature, as summarized in Table II, due to the equilibrium between bis and mono adducts **3b,c**. For example, at 20 °C, decreasing $[\text{CD}_3\text{CN}]$ from 3.5 to 0.69 M causes H_β to shift *upfield* from δ 1.16 to 0.83 and H_α to shift *downfield* from δ 0.87 to 1.08, consistent with the expected shift in equilibrium toward **3b**. From the variation of $\delta(\text{H}_\alpha)$ and $\delta(\text{H}_\beta)$ with $[\text{CD}_3\text{CN}]$ at 20 °C, using the spectrum of **3a** in neat CD_3CN as the reference spectrum for **3c**, and by making a small correction for the effect of changing solvent composition (see Experimental Section), the nitrile dissociation equilibrium constant for eq 5 can be estimated ($K_{\text{eq}} = 0.5(3)$ M) and the chemical shift for the mono(nitrile) adduct **3b** predicted (H_β δ 0.3(1); H_α δ 1.3(6)).²⁷ The latter values are slightly downfield of the values observed for **3b** at −40 °C (Table I). We observed a similar temperature dependence of the ^1H NMR spectrum of **9**.^{5a,15,28}

(25) Complex **12** (CD_2Cl_2 solution) decomposes at 23 °C to a mixture of $\text{Cp}'_2\text{Zr}(\text{Et})\text{Cl}$ and other uncharacterized Zr complexes. The observation of a $\text{Zr}\{\text{N}=\text{C}(\text{H})(\text{R})\}$ resonance at δ 8.5 and ethylene indicates that at least some β -H elimination occurs. This decomposition was not investigated in detail.

(26) At −40 °C, changing $[\text{CD}_3\text{CN}]$ from 0.8 to 3.8 M shifts the THF resonances from δ 3.66 and 1.80 to δ 3.64 and 1.78.

(27) The percentage of **3** present as mono(CH_3CN) adduct **3b** varies from 50% at $[\text{CH}_3\text{CN}] = 0.5$ M to 11% at $[\text{CH}_3\text{CN}] = 4.0$ M.

(28) Other agostic systems exhibit similar temperature-dependent spectra. For example see the data for (dmpe)TiCl₃Et in: Dawoodi, Z.; Green, M. L. H.; Mtetwa, V. S. B.; Prout, K.; Schultz, A. J.; Williams, J. M.; Koetzle, T. F. *J. Chem. Soc., Dalton Trans.* 1986, 1629.

The 1H NMR spectrum of **3b,c** is much less sensitive to $[CD_3CN]$ at $-40^\circ C$. Decreasing $[CD_3CN]$ from 5.5 to 0.7 M shifts the H_β resonance upfield (from δ 1.15 to 1.08) and the H_α resonance downfield (from δ 0.71 to 0.81), although H_β is always downfield of H_α (Table II). These results indicate that the bis(CH_3CN) adduct is more strongly favored at low temperature, as expected on entropic grounds.

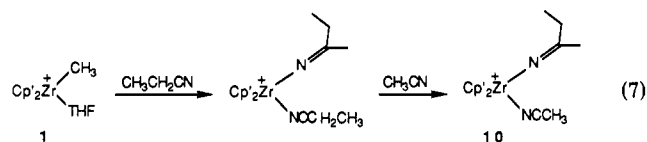
Solution Structures of CH_3CN Adducts **4b,c–**7b,c**.** Isolation of CH_3CN adducts **4b,c**–**7b,c** was precluded by their rapid β -H elimination, though some insight to the behavior of neohexyl system **7** is provided by NMR studies. The NMR spectra of CD_3CN solutions of **7a** exhibit resonances for free THF and significant shifts in the $Cp'_2Zr(CH_2CH_2^tBu)^+$ resonances compared to **7a** in CD_2Cl_2 . The H_β resonance (δ 1.26) is *downfield* of the H_α resonance (δ 0.71), the same relative position as for **7a** in CD_2Cl_2 or THF- d_8 and for **3c**, consistent with the formation of bis(nitrile) adduct **7c** in which the alkyl group has a normal structure. Addition of excess CD_3CN to CD_2Cl_2 solutions of **7a** also results in complete substitution of the THF, as established by the presence of free THF resonances. The H_α and H_β resonances shift significantly as $[CD_3CN]$ is varied, with the latter moving *upfield* of the former at low $[CD_3CN]$.²⁹ This is analogous to the behavior of **3** and is consistent with the equilibrium between **7c** and mono(CD_3CN) adduct **7b** in eq 5. The upfield shift of the β - CH_2 resonance and the observation of an agostic structure for $Cp'_2Zr(CH_2CH_2^tBu)(PMe_3)^+$ (**13**) suggest that **7b** also has an agostic structure. By analogy, the putative mono(CH_3CN) species **4b**–**6b** also likely adopt β -agostic structures.

Structural Trends in $Cp'_2Zr(CH_2CH_2R)(L)_n^+$ Complexes. By analogy to $Cp_2Zr(CH_3)(CH_3CN)_2^+$, $Cp'_2Zr(H)(PMe_3)_2^+$, and related $Cp_2Zr(R)(L)_2^+$ complexes,¹ two isomers are possible for the bis(CH_3CN) complexes **3c**–**7c**: a symmetric isomer with the (normal) alkyl ligand in the central coordination site and an unsymmetric isomer with the alkyl ligand in a lateral site. However, the rapid CH_3CN exchange precluded investigation of this question. Similarly, two isomers which differ in placement of the Zr–H–C interaction (central coordination site, "endo" isomer; lateral site, "exo" isomer) are possible for the β -agostic $Cp'_2Zr(CH_2CH_2R)(L)^+$ species **3b**, **7b**, **9**, **12**, and **13**. The observation of only single sets of resonances in the low-temperature ($-80^\circ C$) NMR spectra of these complexes implies that only a single isomer is present in each case or that isomer interconversion is rapid. One possibility is that isomer exchange is catalyzed by excess nitrile via formation of the bis(nitrile) adducts; this process could occur during the generation of **3b** and **12** from THF complex **3a**.

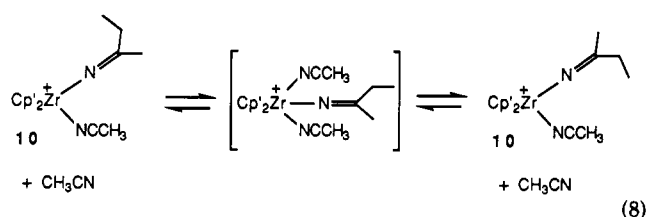
The structural difference between the β -agostic complexes **3b**, **9**, and **12** and the normal complexes **3a** and $Cp'_2Zr(Et)Cl$ is ascribed to π -donation from the THF or Cl^- ligands in the latter, which utilizes the empty metal orbital required for interaction with the β C–H bond. Note that the observation of agostic Zr–H–C structures for the relatively crowded complexes **9**, $Cp'_2Zr(CH_2CH_2^tBu)(PMe_3)^+$ (**13**), and other $Cp'_2Zr(CH_2CH_2R)(PMe_3)^+$ complexes suggests that steric interactions in **3a** would not be sufficient to preclude an agostic structure. A similar structural trend was observed in cationic benzyl complexes $(C_5R_5)_2Zr(CH_2Ph)(L)^+$ ($C_5R_5 = Cp, Cp', EBTHI$).^{3c,5b} The

benzyl ligands are normal in the THF complexes but adopt distorted η^2 structures due to Zr–Ph interactions in the CH_3CN complexes.

Synthesis and Solution Properties of Azaalkenylidene Complexes **10 and **11**.** Azaalkenylidene complex **10**, the product of CH_3CN insertion of $Cp'_2Zr(Et)(CH_3CN)_n^+$, is best synthesized by the reaction of $Cp'_2Zr(CH_3)(THF)^+$ with propionitrile followed by ligand exchange with CH_3CN (eq 7). This synthesis avoids the need to separate **10** from **11** (which is a coproduct in eq 6). Key data for **10** include a low-field imino ^{13}C resonance at δ 183.5, and $\nu_{C=N}$ (1686 cm^{-1}) and $\nu_{C\equiv N}$ ($2300, 2272\text{ cm}^{-1}$) IR absorbances.



The 1H NMR spectrum of **10** in CD_2Cl_2 at $25^\circ C$ contains two sets of Zr=N=C(Et)(Me) and N \equiv CCH $_3$ resonances in a 3:1 ratio. This is consistent with the existence of two isomers which contain Zr=N=C(Et)(Me) ligands lying in the plane between the two Cp' ligands, but which differ by rotation about the Zr=N=C linkage. The in-plane orientation allows Zr–N π -bonding and minimizes steric interactions with the Cp' ligands. Interconversion of the two isomers in CD_2Cl_2 is rapid above $67^\circ C$ (sealed tube experiment!), as indicated by the collapse of the two sets of resonances to a single set. The isomerization is also promoted by excess CD_3CN . Only a single, sharp set of resonances is observed in the 1H NMR spectrum of **10** in CD_3CN solution. The 1H NMR spectrum of **10** in CD_2Cl_2 solution containing 0.5 M CD_3CN exhibits a broad singlet for the N=CCH $_2$ CH $_3$ group at $-40^\circ C$, which sharpens as the temperature or $[CD_3CN]$ is raised. These observations are accommodated by an isomer-exchange process involving a bis(CH_3CN) species (eq 8).



Complex **11** decomposes in neat CH_3CN to as yet uncharacterized products ($t_{1/2}$ ca. 1.2 h, $23^\circ C$).³⁰ However, this decomposition is not significant during the kinetics experiments described below.

Kinetics of the Reaction of **3 with CH_3CN .** The relatively slow rates of reaction of **3** and **7** with CH_3CN (eq 6) permitted detailed kinetic studies. Solutions of CD_3CN adduct **3c-d₆** (in equilibrium with **3b-d₃**) in CD_2Cl_2 were generated in situ in NMR tubes by addition of CD_3CN to solutions of the THF complex **3a**. CD_3CN is used in these experiments to simplify the NMR spectra and to minimize dynamic range problems which make

(30) Azomethine/nitrile complexes undergo C–C coupling processes. (a) Guram, A. S.; Jordan, R. F.; Taylor, D. F. *J. Am. Chem. Soc.* **1991**, *113*, 1833. (b) Bercaw, J. E.; Davies, D. L.; Wolczanski, P. T. *Organometallics* **1986**, *5*, 443. (c) Richeson, D. S.; Mitchell, J. F.; Theopold, K. H. *Organometallics* **1989**, *8*, 2570.

(29) NMR data of **7b,c** in CD_2Cl_2 containing CD_3CN : $[CD_3CN] = 0.68$ M $\delta(H_\alpha)$ 0.95, $\delta(H_\beta)$ 0.89; $[CD_3CN] = 3.18$ M $\delta(H_\alpha)$ 0.82, $\delta(H_\beta)$ 1.13.

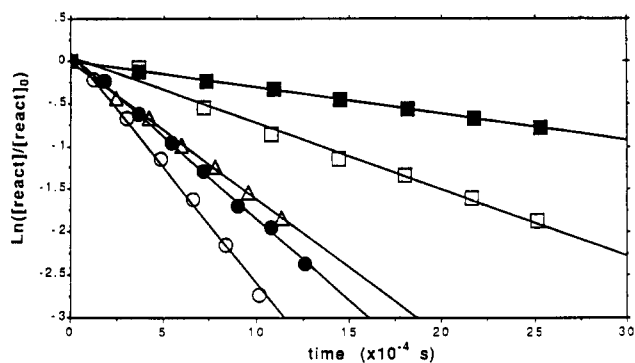


Figure 1. Representative first-order plots for the disappearance of **3**: $[\text{CD}_3\text{CN}]$: (■) 5.45 M; (□) 4.00 M; (△) 1.82 M; (●) 1.01 M; (○) 0.70 M.

Table III. Pseudo-First Order Rate Constants k_{obs} for Reaction of $\text{Cp}'_2\text{Zr}(\text{CH}_2\text{CH}_3)^+$ (**3**) and $\text{Cp}'_2\text{Zr}(\text{CH}_2\text{CH}_2\text{CMe}_3)^+$ (**7**) with CD_3CN (CD_2Cl_2 Solution, $20.0(4)^\circ\text{C}$)^a

entry	complex	$[\text{CH}_3\text{CN}]$, M	$10^{-4}k_{\text{obs}}$, s^{-1}
1	3	0.55	3.57(7)
2	3	0.60	3.07(17)
3	3	0.70	3.16(9)
4	3	1.01	2.35(5)
5	3	1.64	1.98(2)
6 ^b	3	1.82	1.64(3)
7	3	2.26	1.59(6)
8	3	2.34	1.56(15)
9	3	3.26	1.13(3)
10	3	4.00	0.949(23)
11	3	5.45	0.808(8)
12	7	1.04	5.21(33)
13	7	1.24	4.53(9)
14	7	2.83	2.41(3)
15	7	3.57	2.11(7)
16	7	3.76	2.07(8)

^a Solutions of **3b,c** and **7b,c** generated from corresponding THF complexes **3a** and **7a**. ^b **3c** was used as the starting material; i.e. no THF is present.

accurate integration difficult. As discussed above, displacement of THF is complete under these conditions.

Thermolyses were carried out at $20.0(4)^\circ\text{C}$ over a range of $[\text{CD}_3\text{CN}]$ from 0.6 to 5.6 M and monitored by ^1H NMR spectroscopy. At each CD_3CN concentration, the reaction is pseudo first order in $[\text{Zr}]$ as determined by the disappearance of the starting material ($\text{C}_5\text{H}_4\text{CH}_3$ or ZrCH_2CH_3 resonance). Representative first-order plots are shown in Figure 1 and pseudo-first-order rate constants summarized in Table III. Essentially identical results were obtained by monitoring the appearance of product (the $\text{C}_5\text{H}_4\text{CH}_3$ resonances of **10-d**₆ and **11-d**₆ are coincident). The ratio of CD_3CN insertion product **10-d**₆ to β -H elimination product **11-d**₆ (5.3(5)) is independent of $[\text{CD}_3\text{CN}]$ and is constant during the course of each reaction.

The data in Table III confirm that the reaction of **3** is significantly inhibited by added CD_3CN . A 10-fold increase in $[\text{CD}_3\text{CN}]$ from 0.55 M (entry 1) to 5.45 M (entry 11) results in a ca. 77% decrease of k_{obs} . A plot of $1/k_{\text{obs}}$ vs $[\text{CD}_3\text{CN}]$ is linear (Figure 2).

In a control experiment designed to verify that the THF liberated by the in situ generation of **3b,c** does not influence the subsequent chemistry, a THF-free solution of **3c** in CD_2Cl_2 containing 1.8 M CD_3CN was generated as described in the Experimental Section. Thermolysis of this sample yielded **10** and **11** in the same ratio as observed in the presence of THF, and the k_{obs} determined by ^1H

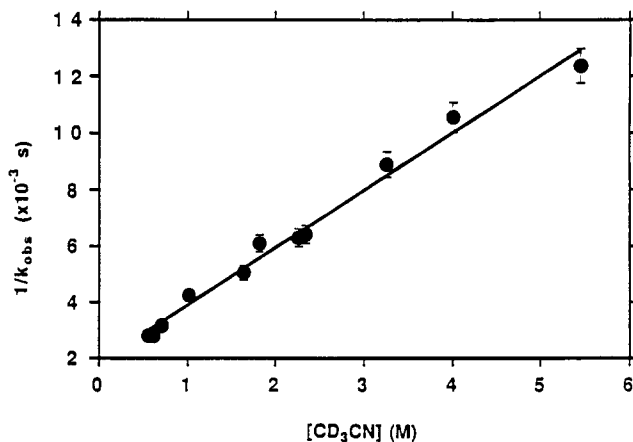
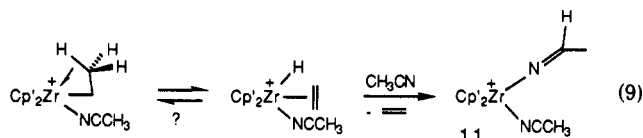


Figure 2. Plot of $1/k_{\text{obs}}$ vs $[\text{CD}_3\text{CN}]$ for **3**. Error bars represent 10% error in $1/k_{\text{obs}}$.

NMR monitoring is close to the value predicted by interpolation of the data in Table III and Figure 2.

Irreversibility of CH_3CN Insertion and β -H Elimination of **3.** There is no evidence for the formation of $\text{Cp}'_2\text{Zr}\{\text{N}=\text{C}(\text{CD}_3)_2\}(\text{CD}_3\text{CN})^+$ or free EtCN in the reaction of **3** with CD_3CN . As both **3b,c** and azaalkenyldene product **10** undergo rapid nitrile exchange, this observation implies that CD_3CN insertion into the $\text{Zr}-\text{Et}$ bond is irreversible.³¹

Careful ^1H NMR monitoring of the reaction of $\text{Cp}'_2\text{Zr}(\text{CH}_2\text{CH}_2\text{D})(\text{CH}_3\text{CN})_n^+$ (**3b,c-d**₁, generated in situ from **3a-d**₁) with CD_3CN under standard conditions (20°C , CD_2Cl_2 containing either high (4.3 M) or low (0.73 M) $[\text{CD}_3\text{CN}]$) reveals that, within experimental error, no deuterium incorporation into the α - CH_2 position of unreacted **3b,c** or the $\text{N}=\text{CCH}_2$ position of the insertion product $\text{Cp}'_2\text{Zr}\{\text{N}=\text{C}(\text{CH}_2\text{CH}_2\text{D})(\text{CD}_3)\}(\text{CD}_3\text{CN})^+$ (**10-d**₇) occurs.³² These results imply that (i) the β -H elimination step is irreversible (i.e. trapping of the $\text{Zr}(\text{H})(\text{olefin})$ species by CH_3CN insertion is faster than the reverse olefin insertion into $\text{Zr}-\text{H}$) or (ii) rotation of coordinated ethylene in the putative ethylene hydride species immediately resulting from β -H transfer is slow (eq 9).³³ An intramolecular isotope effect $k_{\text{H}}/k_{\text{D}} = 2.0(1)$ for the β -H elimination is calculated from the ratio of ethylene products $\text{CH}_2=\text{CH}_2/\text{CH}_2=\text{CHD}$ of the reaction of **3-d**₁ with CD_3CN .



(31) (a) This assumes that the Me and Et groups of $\text{Zr}\{\text{N}=\text{C}(\text{Me})(\text{Et})\}$ species would migrate back to Zr at similar rates in nitrile deinsertion reactions. (b) Stereoselective, reversible alkyl migration to and from the inner or outer azaalkenyldene sites of $\text{Zr}\{\text{N}=\text{C}(\text{R})(\text{R}')\}(\text{NCR})^+$ species is conceivable. However, this is not likely to mask reversible Et migration of **3b,c** as the two isomers of insertion product **10** interconvert rapidly under the reaction conditions.

(32) Integral ratio β - $\text{CH}_2\text{D}/\alpha$ - $\text{CH}_2 = 1.04(5)$ in unreacted **3b,c**; 1.17(8) in product **10-d**₇.

(33) Little is known about olefin rotation barriers in d^0 systems as such systems are unknown. Olefin rotation barriers in d^2 $\text{Cp}_2\text{M}(\text{R})(\text{olefin})$ or $\text{Cp}_2\text{M}(\text{olefin})(\text{L})$ species are high for electronic reasons. (a) Guggenberger, L. J.; Meakin, P.; Tebbe, F. N. *J. Am. Chem. Soc.* 1974, 96, 5420. (b) Green, M. L. H.; Mahtab, R. *J. Chem. Soc., Dalton Trans.* 1979, 262. (c) Benfield, F. W. S.; Cooper, N. J.; Green, M. L. H. *J. Organomet. Chem.* 1974, 76, 49. (d) Alt, H. G.; Denner, C. E.; Thewalt, U.; Rausch, M. D. *J. Organomet. Chem.* 1988, 356, C83. (e) Doherty, N. M.; Bercaw, J. E. *J. Am. Chem. Soc.* 1985, 107, 2670.

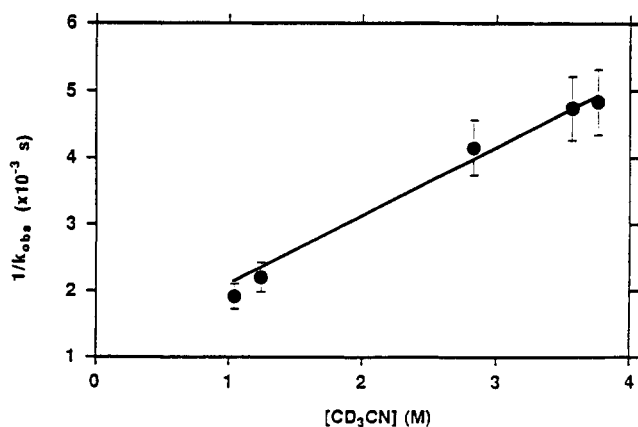
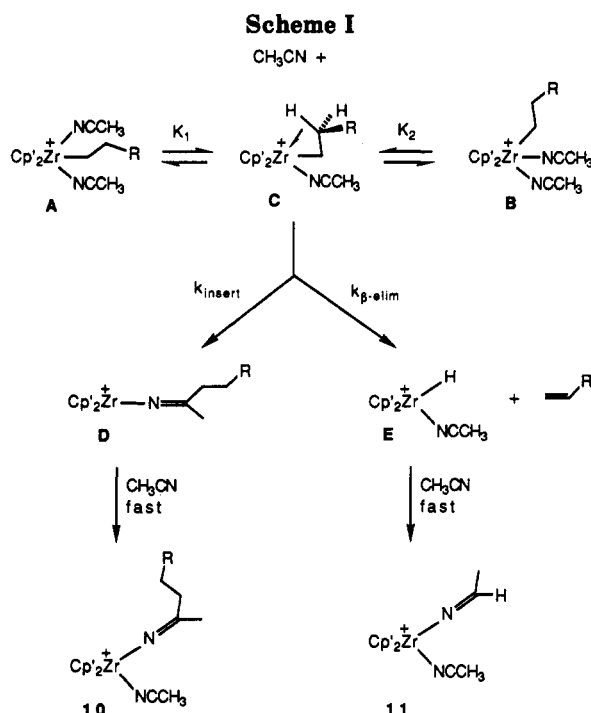


Figure 3. Plot of $1/k_{obs}$ vs $[CD_3CN]$ for **7**. Error bars represent 10% error in $1/k_{obs}$.



Kinetics of the Reaction of 7 with CH_3CN . The kinetics of the reaction of neoheptyl system **7** with CH_3CN were studied using the procedures described above for **3**. Solutions of CD_3CN complex **7b,c-d₃,d₆** in CD_2Cl_2 containing varying $[CD_3CN]$ (1.0–3.8 M) were generated by reaction of **7a** with excess CD_3CN , thermolyzed at 20.0 ± 0.4 °C, and the disappearance of **7b,c-d₃,d₆** was monitored by 1H NMR ($ZrCH_2CH_2^tBu$ resonance). As for **3**, the reaction is pseudo first order in $[Zr]$; values for k_{obs} derived from plots of $\ln [Zr]$ vs time are listed in Table III. This reaction is also inhibited by CD_3CN . Increasing $[CD_3CN]$ from 1.04 M (entry 12) to 3.76 M (entry 16) results in a 60% decrease of k_{obs} . As for **3**, the plot of $1/k_{obs}$ vs $[CD_3CN]$ is linear (Figure 3).

Mechanism for Reactions of 3 and 7 with CD_3CN . The key experimental findings relevant to the mechanism of the reaction of ethyl system **3** with CD_3CN are as follows: (i) The bis(CD_3CN) complex **3c** is in equilibrium with the agostic mono(CD_3CN) adduct **3b** in CD_2Cl_2 solution. Exchange of coordinated and free CD_3CN and exchange of **3c** and **3b** are rapid on the NMR time scale. (ii) The reaction is inhibited by added CD_3CN . (iii) The product ratio 10/11 is independent of $[CD_3CN]$ and is constant

Table IV. Insertion and β -Elimination Rate Constants and CD_3CN Dissociation Equilibrium Constants for **3** and **7** Derived from Kinetic Analysis (20.0(4) °C)

compd	k_{insert}, s^{-1}	$k_{\beta-elim}, s^{-1}$	K_{eq}, M
3b	$4.38(9) \times 10^{-4}$	$8.20(13) \times 10^{-5}$	0.92(13)
7b		$9.4(1) \times 10^{-4}$	1.08(15)

during the reaction. (iv) The insertion pathway leading to **10** and the β -H elimination pathway leading to **11** appear to be irreversible.

These observations are accommodated by the generalized mechanism in Scheme I. In this scheme, the bis(CD_3CN) complex **A** (symmetric) and **B** (unsymmetric) are in equilibrium with mono(CD_3CN) adduct **C**, which has a β -agostic structure. Complex **C** undergoes rate-limiting CD_3CN insertion to form 3-coordinate azaalkenylidene species **D** or β -elimination to form hydride **E**. Intermediate **D** is rapidly trapped by CD_3CN coordination (yielding **10**), and **E** is rapidly trapped by insertion and CD_3CN coordination (yielding **11**).

The rate law for Scheme I under preequilibrium conditions is given by eqs 10–13. The preequilibrium approximation is based on the observed rapid (NMR time scale) exchange between **A**–**C**. Consistent with eq 13, the

$$\text{rate} = \frac{K_{eq}(k_{insert} + k_{\beta-elim})}{K_{eq} + [CD_3CN]} [Zr] = k_{obs} [Zr] \quad (10)$$

$$\text{where } [Zr] = [A] + [B] + [C] \quad (11)$$

$$K_{eq} = \frac{K_1 K_2}{K_1 + K_2} = \frac{[3b][CD_3CN]}{[3c]} = \frac{[B][CD_3CN]}{[A] + [C]} \quad (12)$$

$$\frac{1}{k_{obs}} = \frac{1}{K_{eq}(k_{insert} + k_{\beta-elim})} [CD_3CN] + \frac{1}{k_{insert} + k_{\beta-elim}} \quad (13)$$

$$\frac{k_{insert}}{k_{\beta-elim}} = \frac{10}{11} \quad (14)$$

plot of $1/k_{obs}$ vs $[CD_3CN]$ for **3** is linear (Figure 2). From this plot and the observed product ratio 10/11 (eq 14), values for the composite nitrile dissociation equilibrium constant K_{eq} (eq 12), and the rate constants k_{insert} and $k_{\beta-elim}$ may be derived (Table IV). The K_{eq} value determined in this way (0.92(13) M) is close to the value estimated from the variation of the NMR spectrum of **3** with $[CD_3CN]$ (0.5(2) M). The discrepancy in these values may in part be due to solvent polarity effects.³⁴

The rate law for Scheme I also applies to the reaction of **7** with CD_3CN , although in this case $k_{\beta-elim}$ is very small,

(34) (a) The polarity of CH_2Cl_2/CH_3CN mixed solvents increases as $[CH_3CN]$ is raised. A small rate inhibition by added CH_3CN was observed in the insertion reactions of $(C_5H_4R)_2Zr(CH_3)(CH_3CN)_n^+$ complexes ($R = H, CH_3$, eq 1) and was traced to a solvent effect.⁹ In the present study, the changes in k_{obs} are larger than those observed for the Me systems. For example, over the range $[CH_3CN] = 4\text{--}0.7$ M, k_{obs} for disappearance of **3** increases by a factor of 3.3, while k_{obs} for $Cp^*_2Zr(CH_3)(CH_3CN)_n^+$ insertion increases only by a factor of 1.3. For **3**, a plot of $\ln k_{obs}$ vs $E_T(30)$ (a solvent polarity parameter)^{34b} shows distinct curvature while a similar plot for $Cp^*_2Zr(CH_3)(CH_3CN)_n^+$ was linear. Furthermore, the K_{eq} values for **3** derived from the NMR experiments and the kinetics analysis are in good agreement; this was not the case for $Cp^*_2Zr(CH_3)(CH_3CN)_n^+$. On the basis of these considerations we have not explicitly accounted for solvent polarity effects in the present work. (b) Reichardt, C. *Solvents and Solvent Effects in Organic Chemistry*; VCH: Weinheim, Germany, 1988; Chapter 7 (see also references therein).

as no 11 is detected in the product mixture, and the equilibrium between the bis- and mono(CD_3CN) adducts and the structures of these species are less well-defined. The plot of $1/k_{\text{obs}}$ vs $[\text{CD}_3\text{CN}]$ for 7 is linear (Figure 3) and provides values for K_{eq} and $k_{\beta\text{-elim}}$ which are listed in Table IV. Scheme I also provides an explanation for the observed inhibition of the $\beta\text{-H}$ elimination reactions of 4b,c–6b,c by added CH_3CN , though detailed studies of these reactions were not performed.

Structure/Reactivity Trends in Reactions of $\text{Cp}'_2\text{Zr}(\text{R})(\text{CH}_3\text{CN})_n^+$ Complexes. The observation of CD_3CN insertion of the mono adduct 3b, rather than bis(CD_3CN) adduct 3c, contrasts with the analogous methyl system in which the bis adduct $\text{Cp}'_2\text{Zr}(\text{CH}_3)(\text{CH}_3\text{CN})_2^+$ inserts (eq 1).⁹ The ethyl migration in 3b ($k_{\text{insert}} = 4.38(9) \times 10^{-4} \text{ s}^{-1}$; 20.0(4) °C) is significantly faster than the methyl migration in $\text{Cp}'_2\text{Zr}(\text{CH}_3)(\text{CH}_3\text{CN})_2^+$ (k_{insert} ca. $8 \times 10^{-5} \text{ s}^{-1}$; 30.2(4) °C).^{9,34a} This may reflect the higher metal electrophilicity in the former species, which activates the coordinated CH_3CN for nucleophilic migration of the alkyl ligand. While both species are formally 18-electron species, the second CH_3CN ligand of $\text{Cp}'_2\text{Zr}(\text{CH}_3)(\text{CH}_3\text{CN})_2^+$ is likely a stronger electron donor than the Zr–H–C interaction in 3b.

Ethyl complex 3b undergoes CD_3CN insertion at least 10× faster than neoheptyl complex 7b.³⁵ The origin of this difference is unknown at present. A slower ethylene insertion rate was observed for $\text{Cp}^*_2\text{Sc}(\text{Et})$ vs $\text{Cp}^*_2\text{Sc}(\text{Pr})$ and was ascribed to ground-state stabilization of the former due to a $\beta\text{-agostic}$ interaction.³⁶ However, it is likely that both 3b and 7b adopt agostic structures. One intriguing possibility is that the insertion and $\beta\text{-H}$ elimination rates are influenced by the structure of the reactive mono- (CD_3CN) adducts. In the the exo isomer shown in Scheme I, the Zr–C bond is cis to the coordinated CH_3CN and direct CH_3CN insertion is possible. However, the endo isomer (with the agostic interaction occupying the central site) must undergo isomerization or cleavage of the agostic interaction to achieve the cis orientation of the Zr–C bond and the CH_3CN which is presumed to be required for insertion. The $\beta\text{-agostic}$ ethyl complex $\text{Cp}'_2\text{Zr}(\text{CH}_2\text{CH}_3)(\text{PMe}_3)^+$ (9) adopts the exo structure in the solid state.^{5a} However Bullock has found that the $\beta\text{-agostic}$ dimetalloethane compound $\text{Cp}_2\text{Zr}\{\text{CH}_2\text{CH}_2\text{Ru}(\text{Cp}(\text{PMe}_3)_2)\text{Cl}\}$, which contains a large substituent on the zirconium $\beta\text{-C}$, adopts the endo structure in the solid state.³⁷ Thus, it is possible that endo structures, in which steric interactions between the $\beta\text{-substituents}$ and the Cp' rings are minimized, are preferred for 4–7 and that insertion is thus disfavored. We noted previously that $(\text{C}_5\text{R}_5)_2\text{Zr}(\eta^2\text{-CH}_2\text{Ph})(\text{CH}_3\text{CN})^+$ complexes, which adopt endo structures with Zr–Ph interactions occupying the central coordination site, are resistant to CH_3CN insertion.^{3b,5c,9} We are currently exploring other, more stable $(\text{C}_5\text{R}_5)_2\text{Zr}(\text{CH}_2\text{CH}_2\text{R})(\text{L})^+$ complexes in order to probe the endo/exo isomerism in more detail.

The observation of $\beta\text{-H}$ elimination of 3b rather than 3c is of course reasonable as the latter lacks a vacant low-

lying Zr orbital for H migration. Assuming that K_{eq} values for 4–6 are similar to those for 3 and 7, the qualitative order for the rate of $\beta\text{-H}$ elimination is 4–6 > 7 > 3. The acceleration of $\beta\text{-H}$ elimination by $\beta\text{-alkyl}$ substituents is consistent with Bercaw's studies of Cp^*_2ScR systems and general observations that chain transfer by $\beta\text{-H}$ elimination is generally faster in propene polymerizations than in ethylene polymerizations.³⁶ One reasonable explanation, proposed by Bercaw, is that $\beta\text{-alkyl/aryl}$ substituents stabilize the developing positive charge on the β carbon in the H– migration transition state. In particular, the $\beta\text{-H}$ elimination order for $\text{Cp}^*_2\text{ScCH}_2\text{CH}_2(\text{p-C}_6\text{H}_4\text{X})$ complexes ($\text{X} = \text{NMe}_2 > \text{CH}_3 > \text{CF}_3$) supports this interpretation. Additionally, ground-state stabilization of $\text{Cp}^*_2\text{Sc}(\text{Et})$ by an agostic interaction may inhibit $\beta\text{-H}$ elimination relative to the higher analogues which adopt normal structures.

Experimental Section

All manipulations were performed under an inert atmosphere or under vacuum using a Vacuum Atmospheres drybox or a high-vacuum line. Solvents were purified by initial distillation from an appropriate drying/deoxygenating agent,³⁸ stored in evacuated bulbs, and added to reaction vessels or NMR tubes by vacuum transfer. NMR tubes were attached to the high-vacuum line via needle-valved adaptors. NMR spectra were obtained on Bruker AC-300, WM-360, or AMX-360 instruments. IR spectra (KBr) were recorded on a Mattson Cygnus 25 instrument. Thermolyses were carried out using a VWR (Model 90T) constant-temperature bath. Elemental analyses were performed by Analytische Laboratorien. The following compounds were prepared as described earlier: $[\text{Cp}'_2\text{Zr}(\text{CH}_3)(\text{THF})][\text{BPh}_4]$ (1),⁹ $[\text{Cp}'_2\text{Zr}(\text{CH}_2\text{CH}_2\text{R})(\text{THF})][\text{BPh}_4]$ (R = H (3a), Me (4a), Et (5a), and Ph (6a)), $[\text{Cp}'_2\text{Zr}(\text{H})(\text{THF})][\text{BPh}_4]$, and $[\text{Cp}'_2\text{Zr}\{\text{N}=\text{C}(\text{CH}_3)(\text{H})\}(\text{CH}_3\text{CN})][\text{BPh}_4]$ (11).^{7b} $3a\text{-}^{13}\text{C}_2$ was prepared by reaction of $\text{Cp}'_2\text{Zr}(\text{H})(\text{THF})^+$ with $^{13}\text{CH}_2=^{13}\text{CH}_2$ and used for the preparation of other ^{13}C -labeled ethyl complexes.

$[\text{Cp}'_2\text{Zr}(\text{CH}_2\text{CH}_3)(\text{CH}_3\text{CN})_2][\text{BPh}_4]$ (3c). To a 5-mm NMR tube containing 18 mg of 3a was added 0.5 mL of CH_3CN at -78 °C via vacuum transfer. The cold bath was removed, the tube was warmed to room temperature for ca. 30 s, and the solid dissolved. Volatiles were removed immediately at room temperature. The process was repeated once more to ensure complete removal of THF. CD_2Cl_2 was added at -78 °C via vacuum transfer. Again the solution was warmed to room temperature for ca. 10 s and all the solid dissolved. Volatiles were removed, and the solid was dried under high vacuum at 23 °C for 10 min to give a yellow foam. CD_2Cl_2 and excess CD_3CN were added at -196 °C via vacuum transfer, and the ^1H NMR of the sample was obtained at -40 °C.

$[\text{Cp}'_2\text{Zr}(\text{CH}_2\text{CH}_3)(\text{CH}_3\text{CN})][\text{BPh}_4]$ (3b). To a 5-mm NMR tube containing 20 mg of 3a was added 0.5 mL of CH_3CN at -78 °C via vacuum transfer. The needle valve was opened to vacuum when the cold bath was removed, and the volatiles were rapidly removed, producing a pale yellow solid. This process was repeated to ensure complete removal of THF. CD_2Cl_2 was added at -78 °C. Again the needle valve was opened to the vacuum when the cold bath was removed and the volatiles were rapidly removed under vacuum. The resulting pale yellow solid was dried at room temperature for 30 min. CD_2Cl_2 was added at -78 °C, and the NMR spectra obtained at -40 °C. The solid is only sparingly soluble in CD_2Cl_2 . Addition of excess CH_3CN to 3b yields 3c.

$[\text{Cp}'_2\text{Zr}(\text{CH}_2\text{CH}_3)\{\text{CH}_3\text{CCN}\}][\text{BPh}_4]$ (12). Methylene chloride (0.5 mL) was added by vacuum transfer at -78 °C to a 5-mm NMR tube containing 3a (10 mg) and *tert*-butylnitrile (1.6 μL , 1 equiv). The tube was warmed to 0 °C, and the volatiles were removed under vacuum, producing an orange oil. The addition

(35) (a) From the lack of $\text{Cp}'_2\text{Zr}\{\text{N}=\text{C}(\text{CD}_3)(\text{CH}_2\text{CH}_2\text{tBu})\}(\text{CD}_3\text{CN})^+$ observed in the product mixture (ca. 5% NMR detection limit) and the value for $k_{\beta\text{-elim}}$ derived from the kinetic analysis ($9.4(1) \times 10^{-4} \text{ s}^{-1}$), a limiting value for k_{insert} for 7b can be estimated ($k_{\text{insert}} < 4.7 \times 10^{-5}$). (b) The insertion rates for the other alkyls could not be measured or estimated due to the rapid $\beta\text{-H}$ elimination in these cases.

(36) Burger, B. J.; Thompson, M. E.; Cotter, W. D.; Bercaw, J. E. *J. Am. Chem. Soc.* 1990, 112, 1566.

(37) Bullock, R. M.; Lemke, F. R.; Szalda, D. J. *J. Am. Chem. Soc.* 1990, 112, 3244.

(38) Perrin, D. D.; Armarego, W. L. F.; Perrin, D. R. *Purification of Laboratory Chemicals*, 2nd ed.; Pergamon Press: New York, 1980.

and removal of CH_2Cl_2 was repeated twice. The resulting oil was dried at 0 °C for 30 min, and CD_2Cl_2 (0.4 mL) was added via vacuum transfer at -78 °C. The tube was maintained at -78 °C prior to NMR analysis at -40 °C which revealed the presence of **12** and a trace amount of **3a**. Extensive decomposition occurred upon warming to 23 °C.

[Cp'Zr(CH₂CH₂CMe₃)(THF)](BPh₄) (7a). A solution of **[Cp'Zr(H)(THF)](BPh₄)** in THF, prepared by hydrogenolysis of **1** (1.01 g, 1.54 mmol), was degassed and charged with *tert*-butylethylene (300 Torr). The solution was stirred at 23 °C for 3 h and then degassed. The solution volume was reduced to 5 mL, and a yellow solid precipitated. This material was collected by filtration and washed with cold THF to yield 376 mg of **7** as a yellow solid. Addition of hexane to the filtrate produced an additional 523 mg of **7**, for an overall yield of 70%. The isolated material contained 0.17 equiv of excess THF, as determined by ¹H NMR. Anal. Calcd for C₄₆H₅₅OZr·0.17THF: C, 74.84; H, 7.51; Zr, 12.36. Found: C, 74.42; H, 7.05; Zr, 12.25. **[Cp'Zr(CH₂CHDCMe₃)(THF)](BPh₄) (7a-d₁)** was prepared in the same manner as **7a**, but D₂ was substituted for H₂. ²H NMR (THF-d₃): δ 1.46.

[Cp'Zr(CH₂CH₂CMe₃)(PMe₃)](BPh₄) (13). Complex **13** was generated *in situ* by addition of PMe₃ (1.7 equiv; measured by calibrated gas bulb) via vacuum transfer at -196 °C to a solution of **7a** (10 mg) in 0.5 mL of CD_2Cl_2 in an NMR tube. The tube was maintained at -78 °C, and NMR spectra (Table I) were obtained at -20 °C. The tube was warmed to 20 °C in the NMR probe. ¹H NMR analysis revealed extensive decomposition to *endo*-Cp'Zr(H)(PMe₃)₂⁺, ^{5a}tBu-ethylene, and several minor unidentified Cp'Zr products.

Isotopic Perturbation of Resonance for 13. A slurry of **7a** (10 mg) and **7a-d₁** (12 mg) in 0.4 mL of PMe₃ was prepared at -78 °C and warmed to 23 °C for 2 min. The volatiles were removed under vacuum. CD_2Cl_2 (0.5 mL) and a trace of PMe₃ were added at -78 °C, and the tube was warmed to 23 °C for ca. 2 min to promote the dissolution of the solid. The volatiles were removed, and the resulting solid was dried under vacuum at 23 °C for 10 min. CD_2Cl_2 was added at -78 °C and the tube flame sealed. ¹H NMR spectra were obtained at -90, -60, -30, and 0 °C. Data are summarized in the text.

[Cp'Zr{N=C(CH₃)(CH₂CH₃)}(CH₃CN)](BPh₄) (10). Propionitrile (0.70 mL, 9.8 mmol) was added via vacuum transfer at -78 °C to a solution of **1** (1.00 g, 1.52 mmol) in THF (30 mL). The resulting light orange solution was stirred at 23 °C for 45 h during which time the solution turned bright orange. The reaction mixture was filtered and the filtrate evaporated to dryness under vacuum to yield **[Cp'Zr{N=C(Me)(Et)}(CH₂CH₂CN)](BPh₄)** as an orange brown solid. The solid was dissolved in CH₃CN, and the volatiles were removed under vacuum. This process was repeated three times. Finally, 20 mL of CH₃CN was added at -78 °C. The solution was warmed to room temperature and concentrated to 5 mL, and a cream-colored solid precipitated. The solid was collected by filtration, washed twice with cold CH₃CN, and dried under vacuum overnight (yield 325 mg of **10**). Addition of Et₂O (20 mL) to the filtrate produced another 357 mg of **10**, for a total yield of 66%. Anal. Calcd for C₄₂H₄₅N₂BZr: C, 74.20; H, 6.67; N, 4.12; Zr, 13.42. Found: C, 74.07; H, 6.59; N, 4.03; Zr, 13.60. IR: (KBr) $\nu_{C=N}$ 1690 cm⁻¹, $\nu_{C=N}$ 2300, 2272 cm⁻¹; (Nujol) $\nu_{C=N}$ 1686 cm⁻¹, $\nu_{C=N}$ 2297, 2267 cm⁻¹.

Kinetics. A sample of **3a** (0.015–0.027 mmol) or **7a** (0.014–0.022 mmol) was loaded into a 5-mm NMR tube equipped with a valved adapter. The tube was attached to a high-vacuum line

and evacuated. A calibrated gas bulb was charged with CD₃CN at a known pressure (60–75 mmHg, measured by Hg manometry). The CD₃CN was transferred to the NMR tube under vacuum at -196 °C. CD_2Cl_2 (ca. 0.4 mL) was added via vacuum transfer at -196 °C, and the tube was flame sealed and kept at -78 °C until thermolysis. Thermolyses were carried out at 20.0 ± 0.4 °C in a constant-temperature bath. For each measurement, the sample was removed from the bath and the reaction quenched by rapid insertion of the tube into a -78 °C bath. A ¹H NMR spectrum was recorded at -40 °C. Control experiments established that no reaction occurs at this temperature. After the spectrum was recorded, the sample was removed rapidly from the probe and inserted into the -78 °C bath, and then into the constant-temperature bath at 20 °C where thermolysis was resumed. In this manner, thermolyses were followed for 2–4 half-lives. In each case, the plot of ln [reactant] vs time was linear with slope = -*k*_{obs}. After each reaction, the tube was opened and the solution volume measured by syringe. The concentration of CD₃CN was calculated by assuming ideal gas behavior of CD₃CN. Control experiments described in the preceding paper establish the accuracy of this procedure for determining [CD₃CN].⁹ Kinetics results are summarized in Tables III and IV, and data analysis is described in the text.

In a control experiment to test the effect of THF on the rate of the thermolysis, **3c** was generated *in situ* in the absence of THF. A 5-mm NMR tube was charged with a known quantity of **3a** and evacuated on the vacuum line. CH₃CN was added at -78 °C and the solvent warmed slightly until the solid dissolved. The solvent was removed under vacuum to give a brown oil. The process was repeated to ensure a complete removal of THF. CD_2Cl_2 was added at -78 °C and the tube warmed slightly until all the solid dissolved. Volatiles were again removed under vacuum to ensure complete removal of excess CH₃CN, yielding a yellow solid. Finally, CD₃CN and CD_2Cl_2 were added, the tube was sealed, and the thermolysis was monitored as described above.

Estimation of K_{eq} by NMR Spectroscopy. The K_{eq} value for CD₃CN dissociation of **3c** at 20 °C was determined from the variation of the β-CH₃ ¹H NMR chemical shift as a function of [CD₃CN]. K_{eq} is related to δ by the equation δ_{obs} = δ_{mono} + [CD₃CN](δ_{bis} - δ_{obs})/K_{eq}, where δ_{obs} = observed chemical shift, δ_{mono} = chemical shift of the mono(CD₃CN) adduct **3b**, and δ_{bis} = chemical shift of the bis(CD₃CN) adduct **3c**.³⁹ Solutions of **3a** in CD_2Cl_2 containing different [CD₃CN] were prepared as described in the kinetics section and their ¹H NMR spectra were recorded at 20 °C. The chemical shifts of the BPh₄⁻ and free THF resonances change slightly (+0.05 δ) as [CD₃CN] is varied from 0.69 M to neat CD₃CN. The chemical shift values for **3** were corrected for this change and are listed in Table II. From a plot of δ_{obs} vs (δ_{bis} - δ_{obs})[CD₃CN] using corrected β-CH₃ δ_{obs} values and δ_{bis} = 0.82 (the chemical shift value in neat CD₃CN after correction), K_{eq} = 0.5(3) M and δ_{mono} = 0.3(1).

Acknowledgment. This work was supported by NSF Grant CHE-9022700 and the Exxon Chemical Co. R.F.J. gratefully acknowledges a Sloan Foundation Research Fellowship (1989–1991) and Union Carbide Research Innovation Awards (1989, 1990).

OM9203441

(39) Drago, R. S. *Physical Methods in Chemistry*; W. B. Saunders Co.: London, 1977; p 252.